Structural Engineering and Mechanics, *Vol. 59, No. 3 (2016) 527-537*
DOI: http://dx.doi.org/10.12989/sem.2016.59.3.527

Warping stresses of a rectangular single leaf flexure under torsion

Nghia Huu Nguyen[1], Ji-Soo Kim[2] and Dong-Yeon Lee[*3]

[1]*Faculty of Mechanical Engineering, Nha Trang University, Khanh Hoa Province, Vietnam*
[2]*Research Institute, OSG Korea, Daegu 704-946, Republic of Korea*
[3]*School of Mechanical Engineering, Yeungnam University, Gyeongsan 712-749, Republic of Korea*

(Received June 3, 2015, Revised March 23, 2016, Accepted May 11, 2016)

Abstract. We describe a stress analysis of a single leaf flexure under torsion in which the warping effect is considered. The theoretical equations for the warping normal stress (σ_{xx}) and shear stresses (τ_{xz} and τ_{xy}) are derived by applying the warping function of a rectangular cross-sectional beam and the twist angle equation that includes the warping torsion. The results are compared with those of the non-warping case and are verified using finite element analysis (FEA). A sensitivity analysis over the length, width, and thickness is performed and verified via FEA. The results show that the errors between the theory of warping stress results and the FEA results are lower than 4%. This indicates that the proposed theoretical stress analysis with warping is accurate in the torsion analysis of a single leaf flexure.

Keywords: torsion; warping; warping normal stress; leaf flexure; warping shear stress

1. Introduction

In a precision machine, especially in nano-scanner devices, a single leaf flexure (SLF) is frequently used due to advantages such as easily obtainable uniform spring material, a very low friction characteristic, and smooth motion. Many previous studies have considered the leaf spring with respect to the design of precision devices. For example, a novel design of a scanning unit for atomic force microscopy is presented in (Schitter *et al.* 2008); displacement reduction mechanisms based on the leverage provided by elastic leaf springs and flexure hinges are considered by Hayashi and Fukuda (2012); parallel leaf spring flexures are proposed by Brouwer *et al.* (2013); a nano-positioning stage with the combination of a hinge and a leaf spring with a relatively high resonance frequency and wide scan range is described by Yong *et al.* (2009); a novel rotation scanner for nano-resolution and accurate rotary motion with an L-shaped flexure leaf spring is developed and tested in (Lee *et al.* 2012); the design and analysis of a novel flexure-based mechanism that is capable of performing planar motion with three degrees of freedom is described in (Bhagat *et al.* 2014); deformations of cantilever beams based on higher-order theory are analyzed in (Sun *et al.* 2015) and the displacement of a single-bent leaf flexure under torsion and in bending is presented by Nguyen *et al.* (2015).

*Corresponding author, Professor, E-mail: dylee@ynu.ac.kr

http://www.techno-press.org/?journal=sem&subpage=8 ISSN: 1225-4568 (Print), 1598-6217 (Online)

The torsion analysis of a beam in general or single leaf flexure has received much consideration in recent years. The equations of rotational displacements in torsion are derived by Hayashi and Fukuda (2012), Koseki *et al.* (2002). However, the warping effect was not considered in detail and the formulas used in the stress analysis were not presented. In other studies, the warping effect in torsion has been analysed in (Yang *et al.* 1984, Wang *et al.* 2010, Sapountzakis and Dourakopoulos 2010, Sapountzakis 2012, Kujawa 2011, Erkmen and Mohareb 2006). However, the warping stresses were not mentioned in the publications (Yang *et al.* 1984, Wang *et al.* 2010, Kujawa 2011), the stress field of a bar under nonuniform torsion was mentioned and analyzed by Erkmen and Mohareb (2006), however the numerical example with specific stress calculations was not presented. Thus, according to the previously mentioned primary shear stresses, which express the shear stresses of uniform torsion (Saint-Venant) with the difference that $\theta_x'(x)$ is not constant and to the normal stresses due to warping resulting from the deformation (primary ones), secondary shear stresses result so as to equilibrate the aforementioned normal stresses" of the paper Sapountzakis (2012). And although these stresses were analysed and presented by Sapountzakis and Dourakopoulos (2010), and Sapountzakis (2012); the formulas of these stresses were not applied and verified in detail. The deflections and stresses of a cantilevered single leaf flexure was analysed by Nguyen and Lee (2015); however, the torsion and torsional stresses were not investigated. The rotational displacement due to the warping torsion of a single leaf flexure is presented by Kim *et al.* (2015). However, the stresses were not analyzed. Torsional shear stresses were also analyzed and computed by Sapountzakis and Mokos (2003), Sapountzakis and Tsipiras (2010), Sapountzakis *et al.* (2015), Pilkey (2002); however, stresses were clarified by different approaches. The general theory for analyzing and calculating the warping stress in beam torsion is shown by Pilkey (2002). However, the author only presented the theoretical formulas, which were not applied and verified by another method. So, the warping stress of an SLF under torsion needs to be analyzed.

In this study, we performed a stress analysis of an SLF in torsion with consideration of the warping effect. The normal stress and two principal direction (y, z) uniform shear stresses of the rectangular section are derived. The warping function of a rectangular cross-sectional beam was applied. The results are compared with those from non-warping torsion. A sensitivity analysis over the length, width, and thickness variation is also performed. FEA was used to validate the accuracy of the theoretical analysis. These results suggested for determining the life and also for studying the various stress acting and helping prevent from getting failure under torsion of SLF in nano-scanner design.

2. Generalized modeling of flexure

Fig. 1 shows the model of the SLF used in this study, which consists of a fixed-end, and a free-end that is subjected to a torsional moment T_x. The dimensions of the structure are length l, width b, and thickness t. In this structure, a single leaf spring enables the free end to move smoothly with an appropriate range of travel and no friction, as discussed in (Schitter *et al.* 2008, Brouwer *et al.* 2013, Lee *et al.* 2012, Bhagat *et al.* 2014). When torsion T_x is applied at the free end of the SLF, the rotational displacement due to warping torsion occurs and then the warping stresses appear. Thus, the warping stresses include the warping normal stress σ_{xx} and warping shear stresses τ_{xz} and τ_{xy}.

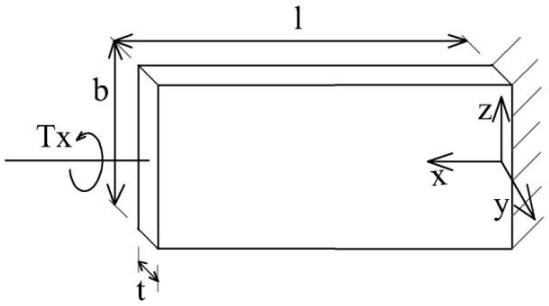

Fig. 1 Schematic diagram of the single leaf flexure

2.1 Warping torsional stress

The governing equation for the non-uniform torsion of a homogeneous isotropic prismatic bar subjected to an end constant torsion T_x with the warping effect was considered, and is given in (Yang *et al*. 1984, Kujawa 2011, Pilkey 2002), including the sum of the St. Venant torsion and the warping torsion as follows

$$GJ_x \frac{d\theta_x}{dx} - EC_w \frac{d^3\theta_x}{dx^3} = T_x \tag{1}$$

The general solution of Eq. (1) is given as follows

$$\theta_x = C_1 + C_2 x + C_3 cosh\alpha x + C_4 sinh\alpha x \tag{2}$$

The applied torsional and warping boundary conditions at both ends of the SLF (freely warping at x=l and fully restrain warping at x=0), the twist angle at the free end of the single bent flexure under torsion load T_x is defined by Kim *et al.* (2015), as follows

$$\theta_x = \frac{T_x}{\alpha G J_x}(\alpha x - sinh\alpha x - tanh\alpha l + tanh\alpha l cosh\alpha x) \tag{3}$$

where $\alpha = \sqrt{\frac{GJ_x}{EC_w}}$ is the torsion-bending constant and C_k (k =1, 2, 3, 4) are the constants of integration. J_x, C_w, G, and E are the torsion constant, warping constant, modulus of transverse elasticity, and modulus of longitudinal elasticity (Young's modulus), respectively.

The torsion constant J_x of the rectangular cross section bar was determined by using Eq. (161) of Timoshenko and Goodier (1951)

$$J_x = \frac{bt^3}{3}\left[1 - 0.63\frac{t}{b}\left(1 - \frac{t^4}{12b^4}\right)\right] \tag{4}$$

The warping constant C_w with respect to the shear center is defined by Eq. (7.43) in Pilkey 2002, as the warping moment of inertia

$$C_w = \int \omega^2 dA = \frac{(bt)^3}{144} \tag{5}$$

From Eq. (3), the first- and second-order derivative equations were determined as follows

$$\theta_x' = \frac{d\theta_x}{dx} = \frac{T_x}{GJ_x}(1 - cosh\alpha x + tanh\alpha l sinh\alpha x) \tag{6}$$

and

$$\theta_x^{"} = \frac{d^2\theta_x}{dx^2} = \frac{\alpha T_x}{GJ_x}(-sinh\alpha x + tanh\alpha l cosh\alpha x) \tag{7}$$

Therefore, the general warping normal stress, and warping shear *XY* and *XZ* stresses, are calculated as follows (Sapountzakis 2012, Sapountzakis and Mokos 2003, Pilkey 2002)

$$\sigma_{xx} = E\frac{d^2\theta_x}{dx^2}\omega(y,z) \tag{8}$$

$$\tau_{xy} = G\frac{d\theta_x}{dx}\left(\frac{\partial\omega}{\partial y} - z\right) \tag{9}$$

$$\tau_{xz} = G\frac{d\theta_x}{dx}\left(\frac{\partial\omega}{\partial z} + y\right) \tag{10}$$

where $\omega(y,z)$ is the warping function. In this study, the warping function of a rectangular cross-sectional beam (Pilkey 2002) was applied as follows

$$\omega(y,z) = yz - \sum_{n=1,3,5}^{\infty} c_n sin\left(\frac{n\pi}{t}y\right) sinh\left(\frac{n\pi}{t}z\right) \tag{11}$$

Where

$$c_n = (-1)^{(n-1)/2}\frac{8t^2}{n^3\pi^3}\frac{1}{cosh(n\pi b/2t)} \tag{12}$$

By substituting Eqs. (6), (7), (11), (12) into Eqs. (8)-(10), the warping normal stresses are given as

$$\sigma_{xx} = \frac{\alpha E T_x}{GJ_x}(-sinh\alpha x + tanh\alpha l cosh\alpha x)\left(yz - \sum_{n=1,3,5}^{\infty} c_n sin\left(\frac{n\pi}{t}y\right) sinh\left(\frac{n\pi}{t}z\right)\right) \tag{13}$$

The maximum warping normal stress ($\sigma_{xx,max}$) occurs at x=0, y=t/2, z=b/2 and is obtained as

$$\sigma_{xx,max} = \frac{\alpha E T_x}{GJ_x}(tanh\alpha l)\left(\frac{tb}{4} - \sum_{n=1,3,5}^{\infty} c_n sin\left(\frac{n\pi}{2}\right) sinh\left(\frac{n\pi b}{2t}\right)\right) \tag{14}$$

From the Eq. (14), we can see that the maximum normal stress ($\sigma_{xx,max} = f\big(sinh(l,b,t)\big)$) is nonlinearly related to l, b and t. Figs. 2(a)-(b) show $\sigma_{xx,max}$ with T_x=1 N·mm, l=10 mm, b=4 mm, t=0.5 mm, assuming that the SLF was made of aluminum 6061 with n=9.

The warping shear stress (τ_{xy}) is given as

$$\tau_{xy} = \frac{T_x}{J_x}(1 - cosh\alpha x + tanh\alpha l sinh\alpha x)\left(\frac{n\pi}{t}\right)\left(\sum_{n=1,3,5}^{\infty} c_n cos\left(\frac{n\pi}{t}y\right) sinh\left(\frac{n\pi}{t}z\right)\right) \tag{15}$$

The value of τ_{xy} occurring at $x = l/2$, $y = 0$ and $z = b/2$ is written as

$$\tau_{xy} = \frac{n\pi}{t}\frac{T_x}{J_x}\left(1 - cosh\left(\frac{\alpha l}{2}\right) + tanh\alpha l sinh\left(\frac{\alpha l}{2}\right)\right)\left(\sum_{n=1,3,5}^{\infty} c_n sinh\left(\frac{n\pi b}{2t}\right)\right) \tag{16}$$

Similarly to the warping normal stress, from the Eq. (16), the warping shear stress ($\tau_{xy} = f\big((l,b,t)\big)$) is nonlinearly related to l, b and t, as shown in Fig. 2(c).

The warping shear stress (τ_{xz}) is given as

$$\tau_{xz} = \frac{T_x}{J_x}(1 - cosh\alpha x + tanh\alpha l sinh\alpha x)\left(2y - \left(\frac{n\pi}{t}\right)\sum_{n=1,3,5}^{\infty} c_n sin\left(\frac{n\pi}{t}y\right) cosh\left(\frac{n\pi}{t}z\right)\right) \tag{17}$$

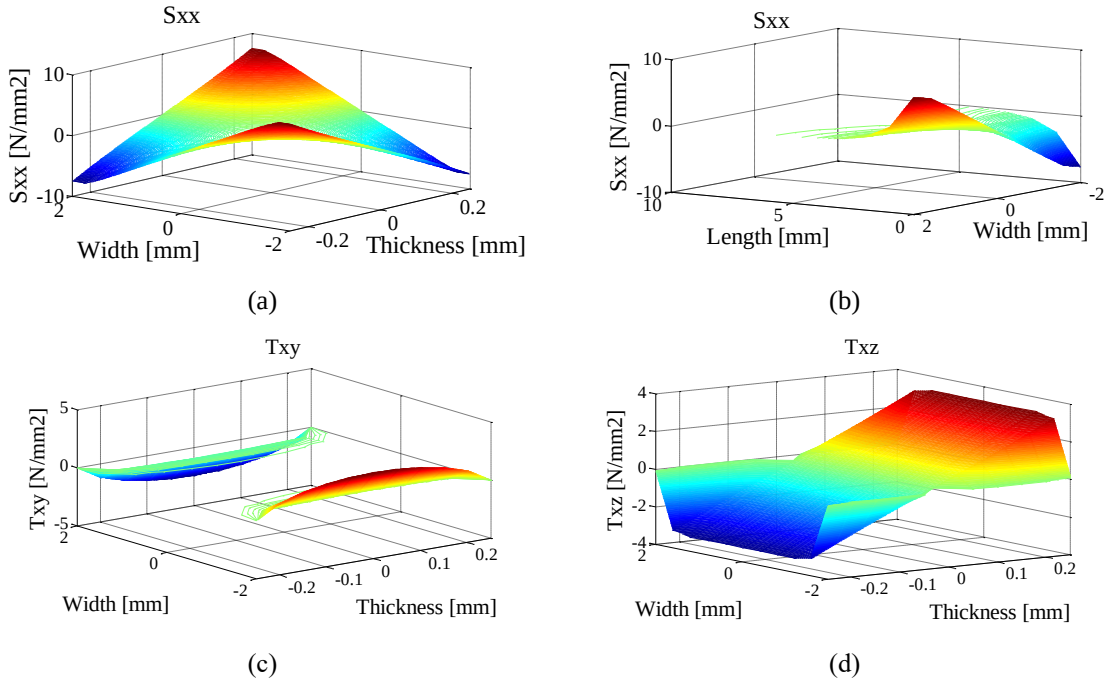

Fig. 2 Maximum warping stresses in the SLF under torsion

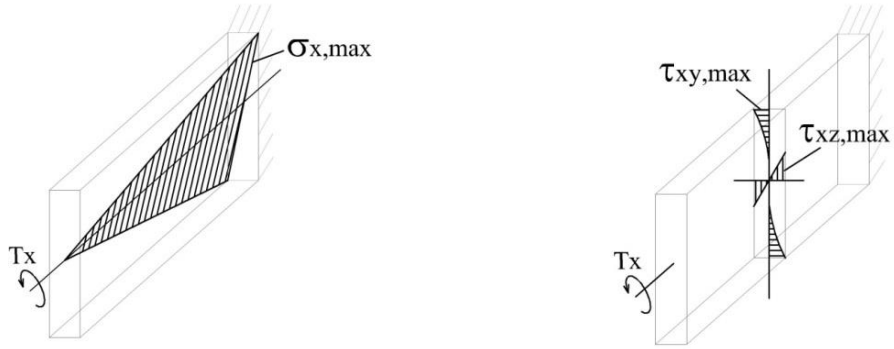

Fig. 3 Maximum stresses in the SLF under torsion

The value of τ_{xz} occurring at $x= l/2$, $y=t/2$ and $z=0$ is written as

$$\tau_{xz} = \frac{T_x}{J_x}\left(1 - cosh\left(\frac{\alpha l}{2}\right) + tanh\alpha l sinh\left(\frac{\alpha l}{2}\right)\right)\left(t - \left(\frac{n\pi}{t}\right)\sum_{n=1,3,5}^{\infty} c_n sin\left(\frac{n\pi}{2}\right)\right) \tag{18}$$

From the Eq. (18), the warping shear stress ($\tau_{xz} = f((l, b, t))$) is nonlinearly related to l, b and t as shown in Fig. 2(d).

Eqs. (14), (16), and (18) show the warping stresses of the SLF under torsion for the case in which the warping effect was considered. The maximum stresses are simply illustrated as in the Fig. 3.

2.2 Non-warping torsional stress

According to the non-wapring torsion theory, the twist angle at the end of a beam under torsion load T_x is given by

$$\theta_x^0 = \frac{T_x x}{G J_x} \tag{19}$$

Therefore, the normal stress is equal to zero. The shear stresses are given by

$$\sigma_{xx}^0 = 0 \tag{20}$$

$$\tau_{xy}^0 = G \frac{d\theta_x}{dx} z \tag{21}$$

$$\tau_{xz}^0 = G \frac{d\theta_x}{dx} y \tag{22}$$

3. Finite element analysis

FEA was conducted by using ANSYS 14.5 commercial FEA software (PA 15317, USA) to verify the results of the theoretical method. The default values of the SLF are as follows: length l=10 mm, width b=4 mm, and thickness t=0.5 mm. We performed a parametric analysis wherein the sensitive parameters were used to check the agreement between the FEA results and theory results, with the following variations: length l=5 to 20 mm, width b=2 to 8 mm and thickness t=0.25 to 1 mm. The torsion moment is T_x=1 N mm. The material used in this simulation is aluminum 6061 with a mesh size of 0.05 mm (hexahedral element), is shown as in Fig. 4. In this study, the stresses of the SLF were found by using FEA and theory, with and without the warping effect, with torsion moment T_x applied at the free end. We then compared these results. If the error between the two methods was lower than 10%, then the results were generally accepted and used in the subsequent design steps.

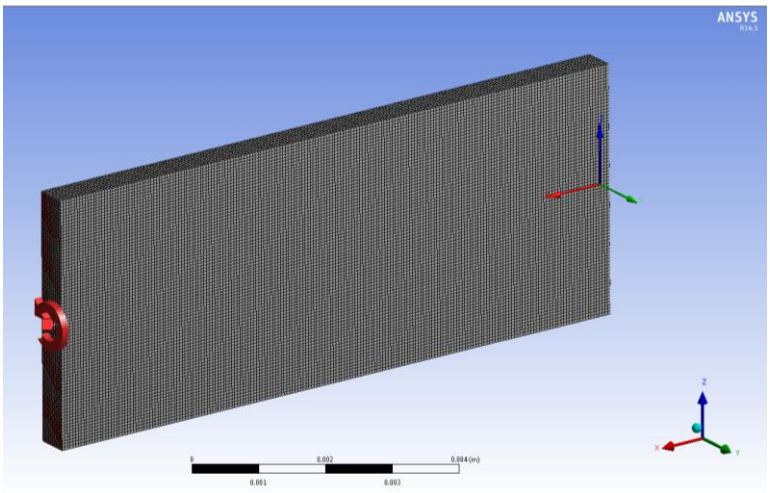

Fig. 4 FEA model of SLF with the employed mesh 0.05 mm

Table 1 Comparison between theory and FEA results at the default values of flexure

	Theory		FEA	Error (%)	
	Warping	Non-warping		Warping	Non-warping
Normal stress σ_{xx} (N/mm^2)	4.5061	0	4.4538	1.16	-
Shear stress τ_{xz}, (N/mm^2)	3.2376	1.6282	3.2458	0.25	49.84
Shear stress τ_{xy} (N/mm^2)	2.4005	13.0257	2.4108	0.43	81.49

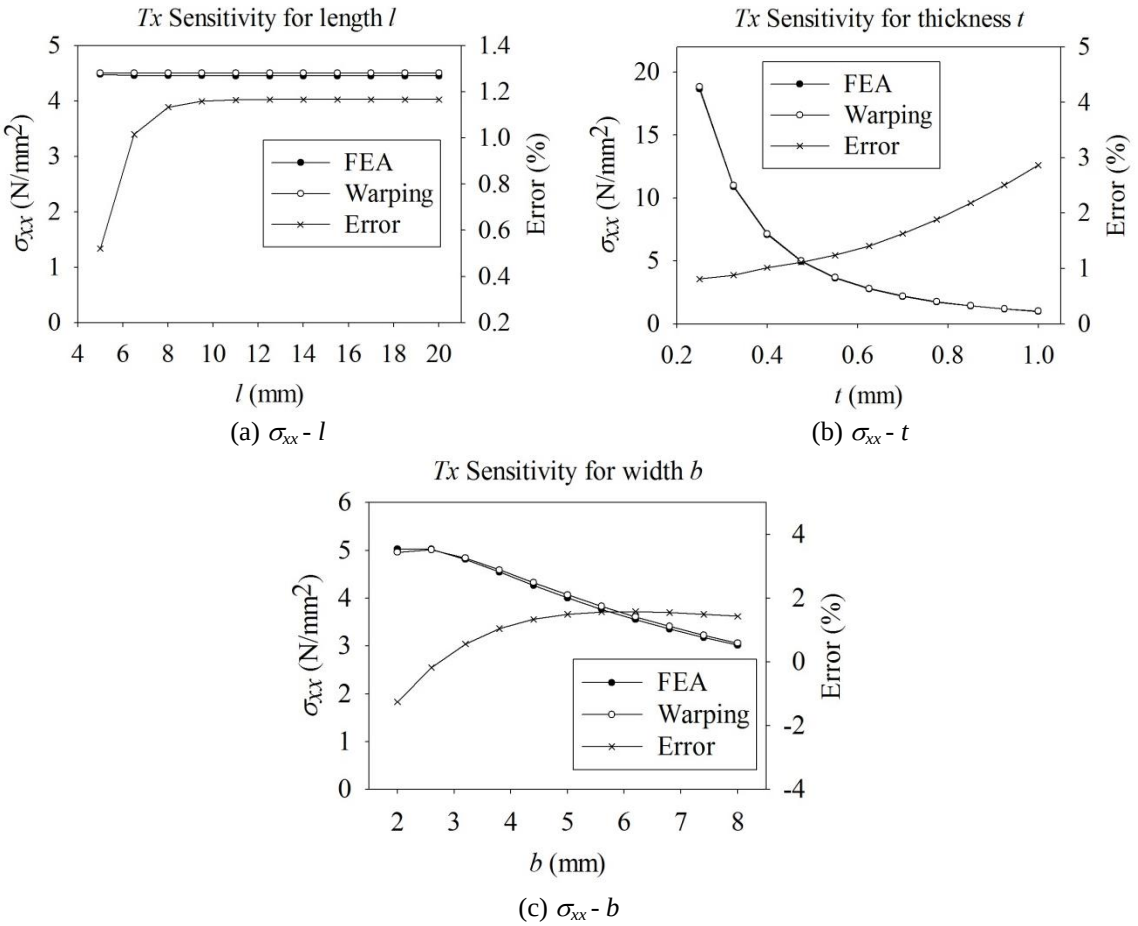

Fig. 5 Variation of warping normal stress σ_{xx} versus (a) length *l,* (b) thickness *t,* and (c) width *b* under torsion T_x

3.1 Comparison at default values

Eqs. (14), (16), and (18) were used to find the stresses of the SLF under T_x with the warping effect. Eqs. (20)-(22) were used to find stresses with no warping effect. The FEA simulation was also conducted at the default values of flexure. Table 1 shows a comparison between the theory (with and without warping) and FEA results (the normal stress (σ_{xx}) was found at x=0, y=t/2, z=b/2; the shear stress (τ_{xy}) was found at x=l/2, y=0, z=b/2; the shear stress (τ_{xz}) was found at x= l/2,

$y=t/2$, $z=0$). As shown in Table 1, the error for warping was lower, at 1.2%, and the errors for non-warping were as high as 82%. Thus, when the warping effect is considered in torsion, the cross-section of the SLF does not remain plane, and is warped into a non-planar surface. Therefore, the normal stress is presented, and the result of stresses due to torsion T_x are quite close to the FEA result. In contrast, the assumption of the classical theory is that the cross-section of the SLF remains plane (no warping), and the results show high errors. This indicates that the stress equation considering warping is in good agreement with the FEA results, and that these results could be accepted for use in subsequent investigations. However, to ensure the reliability of the calculations, the sensitive parameters need to be analyzed.

3.2 Sensitive parameter analysis

Figs. 5(a)-(c) show the simulation results for the warping normal stress σ_{xx} sensitivity with variations of length l=5 to 20 mm (Fig. 5(a)), thickness t=0.25 to 1 mm (Fig. 5(b)), and width b=2 to 8 mm (Fig. 5(c)) of the SLF under torsion T_x. The curves of the variation of warping normal stress σ_{xx} are similar to those from FEA. And, these figures show the curves of the errors. All errors are lower than 3%, which means that the theory results are in good agreement with the FEA results. In these simulations, the non-warping normal stress is considered to be σ^0_{xx}=0.

Figs. 6(a)-(c) show the results of the variation in warping shear stress τ_{xz} according to length l=5 to 20 mm (Fig. 6(a)), thickness t=0.25 to 1 mm (Fig. 6(b)), and width b=2 to 8 mm (Fig. 6(c)) of the SLF based on theory (warping and non-warping) and FEA. We note that the curves of the variation of warping and FEA are quite similar, whereas the curve of the non-warping case differs. The curves of the errors show more clearly the difference: the error of the warping case is lower by 4%, and the other case is up to 50%.

Similarly, Figs. 7(a)-(c) show the simulation results for the warping shear stress τ_{xy} sensitivity with the variation of length l=5 to 20 mm (Fig. 7(a)), thickness t=0.25 to 1 mm (Fig. 7(b)), and width b=2 to 8 mm (Fig. 7(c)) of the SLF under torsion T_x. The curves representing the variation of τ_{xy} show a huge difference in the values of the cases with and without the warping effect. The

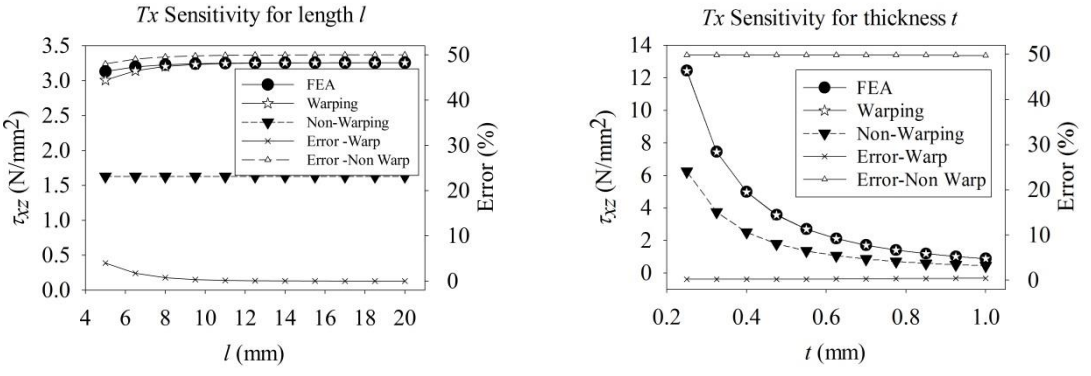

(a) τ_{xz} - l (b) τ_{xz} - t

Fig. 6 Variation of warping shear stress τ_{xz} versus (a) length l, (b) thickness t, and (c) width b under torsion T_x

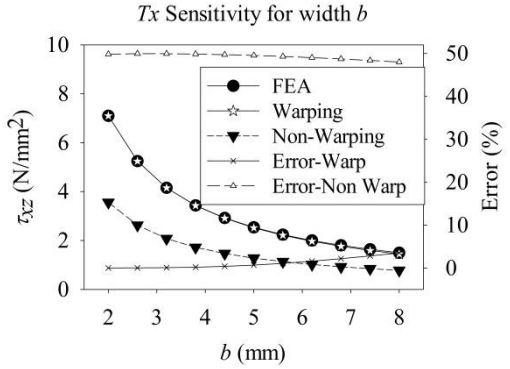

(c) τ_{xz} - b

Fig. 6 Continued

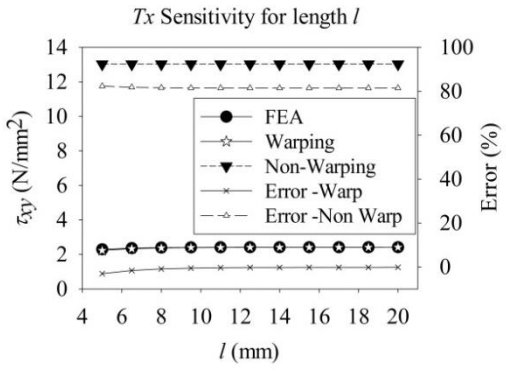

(a) τ_{xy} - l

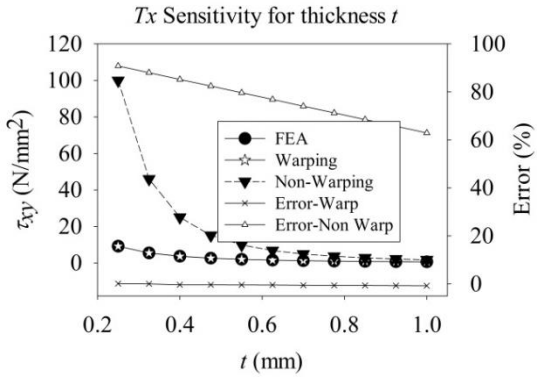

(b) τ_{xy} - t

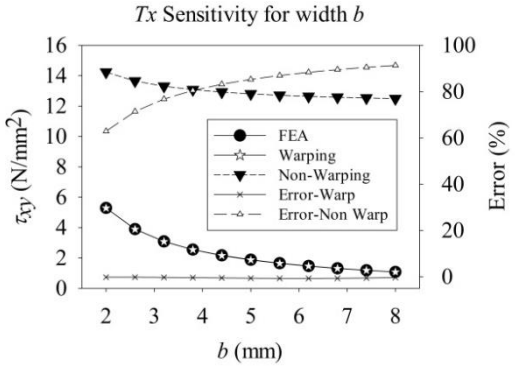

(c) τ_{xy} - b

Fig. 7 Variation of warping shear stress τ_{xy} according to (a) length l, (b) thickness t, and (c) width b under torsion T_x

errors in the warping effect sensitivity with FEA are lower by 3%, and the errors in the non-warping case are up to 92%. These graphs show that the theory results with the warping effect are in strong agreement with the results of FEA.

The warping and non-warping results are compared with FEA as shown in Figs. 5-7. The errors in the warping sensitivity analysis are lower than 4%. The non-warping errors are 92%. These results indicate that the stress analysis of the SLF considering the warping effect in torsion ensures the accuracy than without the warping effect. The normal stress existed during the application of torsion.

4. Conclusions

In this study, the stresses of an SLF with warping and non-warping effects under torsion were analyzed. The warping function of a rectangular cross-sectional beam was applied. The equations of warping normal stress and two shear stresses were derived. A sensitivity analysis with the variation of parameters of the SLF was performed, and the accuracy of the theoretical analysis was validated by FEA. These results show that the proposed analysis with warping in torsion has high accuracy and could be applied to the design of precision machines.

Acknowledgments

This work was supported by the 2015 Yeungnam University Research Grant.

References

Bhagat, U., Shirinzadeh, B., Clark, L., Chea, P., Qin, Y., Tian, Y. and Zhang, D. (2014), "Design and analysis of a novel flexure-based 3-DOF mechanism", *Mech. Mach. Theor*., **74**, 173-187.

Brouwer, D.M., Meijaard, J.P. and Jonker, J.B. (2013), "Large deflection stiffness analysis of parallel prismatic leaf-spring flexures", *J. Precis. Eng*., **37**, 505-521.

Erkmen, R.E. and Mohareb, M. (2006), "Torsion analysis of thin-walled beams including shear deformation effects", *Thin Wall Struct*., **44**, 1096-1108.

Hayashi, M. and Fukuda, M. (2012), "Generation of nanometer displacement using reduction mechanism consisting of torsional leaf spring hinges", *Int. J. Precis. Eng. Man*., **13**(5), 679-684.

Kim, J.S., Lim, B.D. and Lee, D.Y. (2015), "Compliance matrix of a single leaf flexure", submitted to *Acta Mechanica.*

Koseki, T.T.Y., Arai, T. and Koyachi, N. (2002), "Kinematic analysis of translational 3-DOF micro parallel mechanism using matrix method", *Adv. Robotics*., **16**(3), 251-264.

Kujawa, M. (2011), "Torsion of restrained thin-walled bars of open constraint bisymmetric cross-section", *Tast quarterly*, **16**(1), 5-15.

Lee, M.Y., Park, E.J., Yeom, J.K., Hong, D.P. and Lee, D.Y. (2012), "Pure nano-rotation scanner", *Adv. Mech. Eng*., **2012**, Article ID 962439, 1-11.

Nguyen, N.H. and Lee, D.Y. (2015), "Bending analysis of a single leaf flexure using higher-order beam theory", *Struct. Eng. Mech*., **53**(4), 781-790.

Nguyen, N.H., Lim, B.D. and Lee, D.Y. (2015), "Displacement analysis of a sngle-bent leaf flexure under transverse load", *Int. J. Precis. Eng. Man*., **16**(4), 749-754.

Nguyen, N.H., Lim, B.D. and Lee, D.Y. (2015), "Torsional analysis of a single-bent leaf flexure", *Struct. Eng. Mech.*, **54**(1), 189-198.

Pilkey, W.D. (2002), *Analysis and design of elastic beams: computational methods*, John Wiley & Sons Inc. New York, USA

Sapountzakis, E.J. (2012), "Bars under torsional loading: a generalized beam theory approach", *ISRN Civil Eng*., **2013**, 1-39.
Sapountzakis, E.J. and Dourakopoulos, J.A. (2010), "Shear deformation effect in flexural-torsional buckling analysis of beams of arbitrary cross section by BEM", *Struct. Eng. Mech*., **35**(2), 141-173.
Sapountzakis, E.J. and Mokos, V.G. (2003), "Warping shear stresses in nonuniform torsion of composite bars by BEM", *Comput. Meth. Appl. Mech. Eng*., **192**, 4337- 4353.
Sapountzakis, E.J. and Tsipiras, V.J. (2010), "Warping shear stresses in nonlinear nonuniform torsional vibrations of bars by BEM", *Eng. Struct*., **32**, 741-752.
Sapountzakis, E.J., Tsipiras, V.J. and Argyridi, A.K. (2015), "Torsional vibration analysis of bars including secondary torsional shear deformation effect by the boundary element method", *J. Sound Vib.*, **355**, 208-231.
Schitter, G., Thurner, P.J. and Hansma, P.K. (2008), "Design and input-shaping control of a novel scanner for high-speed atomic force microscopy", *Mechatronics*, **18**(2008), 282-288.
Sun, Z., Yang, L. and Yang, G. (2015), "The displacement boundary conditions for Reddy higher-order shear cantilever beam theory", *Acta Mech*., **226**, 1359-1367.
Timoshenko, S.P. and Goodier, J.N. (1951), *Theory of Elasticity*, McGraw-Hill Book Company, New York, USA.
Wang X.F., Yang Q.S. and Zhang Q.L. (2010), "A new beam element for analyzing geometrical and physical nonlinearity", *Acta Mech*., **26**, 605-615.
Yang, Y.B. and McGuire, W. (1984), "A procedure for analysing space frames with partial warping restraint", *Int. J. Numer. Meth. Eng*., **20**, 1377-1398.
Yong, Y.K., Aphale, S.S. and Moheimani, S.O.R. (2009), "Design, identification, and control of a flexure-based XY stage for fast nanoscale positioning", *IEEE T. Nanotechnol.*, **8**(1), 46-54.

CC